ECOHYDROLOGY
Ecohydrol. (2011)
Published online in Wiley Online Library
(wileyonlinelibrary.com) DOI: 10.1002/eco.254

Spatial variability of remotely sensed soil moisture in a temperate-humid grassland catchment

Wen Liu,[1] Xianli Xu[1,2]* and Gerard Kiely[1]

[1] *Centre for Hydrology, Micrometeorology and Climate Change, Department of Civil and Environmental Engineering, University College Cork, Cork, Ireland*
[2] *Center for Sustainable Water Resources, Bureau of Economic Geology, Jackson School of Geosciences, The University of Texas at Austin, TX, 78758, USA*

ABSTRACT

Knowledge of the spatial distribution of soil moisture is very important for understanding eco-hydrological processes, but monitoring of soil moisture over extensive areas remains a challenge because of its high spatial variability and temporal dynamics. This study, taking an Irish temperate-humid catchment as an example, shows that the backscatter coefficient acquired from Environmental Satellite (ENVISAT) Advanced Synthetic Aperture Radar (ASAR) Wide Swath (WS) image (150 m resolution) is a good estimator of the surface (top 5 cm) soil moisture, leading us to propose an empirical model for soil moisture estimation. Statistical analysis of the remotely sensed soil moisture (produced from 35 ENVISAT/ASAR WS images spanning both wet and dry regimes in 2006) revealed that the spatial variation (standard deviation and coefficient of variance) mainly decreased with increasing mean soil moisture for this wet catchment. Geostatistical analysis showed that the spatial dependence of the soil moisture field was moderate with most of the nugget ratios ranging from 45% (25% percentile) to 55% (75% percentile), and the spatial correlation range was around 554–854 m. The exponential model was able to accurately fit the sample semivariograms and was a reliable estimator of the characteristics of the remotely sensed soil moisture field. This type of analysis can provide meaningful information for soil moisture monitoring at the catchment or regional scale. Copyright © 2011 John Wiley & Sons, Ltd.

KEY WORDS soil moisture; remote sensing; ENVISAT/ASAR; backscatter coefficient; spatial variability

Received 4 October 2010; Revised 21 July 2011; Accepted 22 July 2011

INTRODUCTION

Soil moisture plays a fundamental role in the soil–atmosphere interactions and eco-hydrological processes (Rodriguez-Iturbe *et al*., 1995; Albertson and Kiely, 2001; Montaldo *et al*., 2001; Bell *et al*., 2010; Koster *et al*., 2010; Pumo *et al*., 2010; Teuling *et al*, 2010; Tietjen *et al*., 2010). Knowledge of soil moisture at the catchment scale is critical for such applications as regional resource management during times of flood or drought and surface soil moisture is a key forcing variable in many Soil-Vegetation-Atmosphere-Transfer models (Moran *et al*., 2006). However, *in situ* monitoring soil moisture at the watershed scale is time-consuming and costly because of its high spatial variability and temporal dynamics.

Because of the large scale and frequent coverage, remote sensing technologies from satellite measurements (e.g. Advanced Microwave Scanning Radiometer-EOS (AMSR-E), Advanced Scatterometer (ASCAT) and Soil Moisture and Ocean Salinity (SMOS)) have been receiving more and more attention in retrieving and monitoring soil moisture in recent years, but most of these measurements are still at a coarse resolution (25–50 km) and also need more validation (Jackson *et al*., 2010). The recent synthetic aperture radar sensors, such as Environmental Satellite (ENVISAT) Advanced Synthetic Aperture Radar (ASAR), offer excellent opportunities to derive land surface parameters (e.g. soil moisture and roughness) from image data, with high spatial resolution (hundreds of meters to several kilometers) and temporal repetition (a few days) covering large areas. Previous studies (Zribi *et al*., 2005; Loew *et al*., 2006; Baup *et al*., 2007a,b; Pathe *et al*., 2009; Mladenova *et al*., 2010; Zribi *et al*., 2010) have shown that the backscatter coefficient acquired from ENVISAT/ASAR is a fairly good estimator of surface soil moisture. However, most of these studies focused on the development of retrieving algorithms, with few on its application for analysis of the spatial variability of soil moisture (e.g. Jacobs *et al*., 2010). The analysis of spatial variability would not only facilitate checking the applicability of the remote sensing techniques but also provide useful information for designing reasonable ground monitoring experiments on surface soil moisture so as to calibrate or validate the existing retrieval models with sufficient *in situ* measurements thereby promoting the models' enhancements (Jackson *et al*., 2010). In addition, the knowledge of soil moisture spatial variability is also helpful in the application of the eco-hydrological models (Mahanama *et al*., 2008; Koster *et al*., 2010; Tietjen *et al*., 2010).

This study uses an Irish temperate-humid catchment as an example, to investigate (1) the applicability of the

*Correspondence to: X. Xu, Center for Sustainable Water Resources, Bureau of Economic Geology, Jackson School of Geosciences, The University of Texas at Austin, J.J. Pickle Research Campus, Bldg. 130, 10100 Burnet Rd., Austin, TX 78758, USA.
E-mail: xuxianliww@gmail.com

ENVISAT/ASAR in retrieving soil moisture for a wet environment, and (2) the spatial variability of the remotely sensed soil moisture at the catchment scale.

MATERIALS AND METHODS

Study area and ground measurements of soil moisture

The study area is an upland sub-catchment, named Dripsey, located in the south west of Ireland covering an area of 15 km^2 at an elevation ranging from 68 to 251 m (Figure 1). The land cover is uniformly agricultural grassland for dairy and beef production. Old Red Sandstone underlies the entire area with overlying soils of peaty gleys on brown podzols. Broadly, the soil is classified as loam in the U.S. Department of Agriculture texture classification. Averaged over the top 10 cm, the soil porosity is 0.60, the saturation moisture level is 0.57, the field capacity is 0.32 and the wilting point is 0.12 $m^3\,m^{-3}$; the pH is 6.7, the soil organic carbon has a mean value of 4.5% and the soil organic N is 0.35%. The climate is temperate and humid with mean annual precipitation (over 10 years) in the region of about

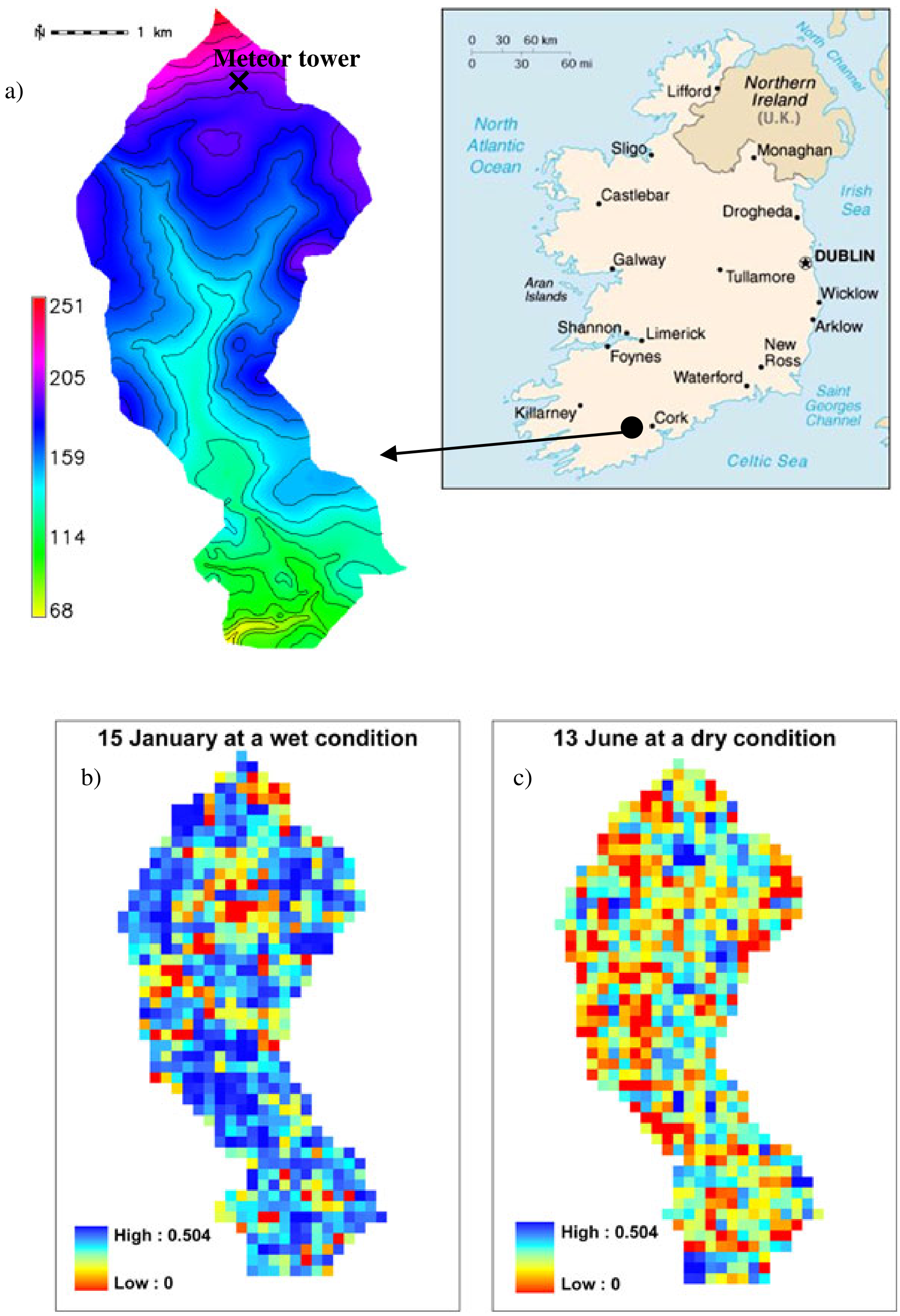

Figure 1. a) Location and contour map (elevation in meters) of the Dripsey catchment showing the location of the meteorological tower (soil moisture monitoring site), b) the simulated soil moisture for a wet condition (Julian day 15 in 2006) and c) the simulated soil moisture for a dry condition (Julian day 164 in 2006).

1470 mm year^{-1} (~1363 mm in 2006). The rainfall regime is characterized by long duration events of low intensity (maximum value up to 50 mm day^{-1}). Short duration events of high intensity are more seldom and occur in summer. Daily air temperatures have a very small range during the year going from a maximum of ~20 °C in summer to a minimum of ~0 °C in winter. The daily summer average is ~15 °C, and the daily winter average is ~5 °C. A time-domain reflectometry probe (Campbell Sci., Logan, UT, USA) at the meteorological tower site (Figure 1) was used to measure the soil moisture at the top 5 cm, and the data were recorded every 30 min. Detailed descriptions about the study area and the meteorological monitoring can be found in the study by Scanlon and Kiely (2003), Scanlon *et al*. (2004), and Kim *et al*. (2010). The soil moisture values at the time closest to the satellite passing time (Table I) were extracted to develop a relationship between the *in situ* soil moisture and the backscatter coefficient from remote sensing images (as described in the following section).

Satellite data sets

ENVISAT/ASAR Wide Swath (WS) mode with a spatial resolution of 150 m (http://envisat.esa.int) was selected for this study. There are 36 images for the year 2006, corresponding to different Julian days (see Table I). The image on Julian day 339 (5 December 2006) was only used for the development of the soil moisture retrieval model, but it was not used for later analysis because of its low quality in some parts of the study area. The software-BEST (Basic Envisat SAR Toolbox 4.0.5.) was used to automatically calibrate and calculate the backscatter coefficients (for details refer to the website: http://envisat.esa.int). The backscatter coefficient of the pixel closest to the ground monitoring site (Figure 1) for each image was selected to develop the relationship between the backscatter coefficient and soil moisture.

Terrain data sets

Two commonly used terrain indices closely associated with soil moisture were calculated based on the 150 m resolution Digital Elevation Model (DEM) (re-sampled from 10 to 150 m in order to match the ENVISAT/ASAR images).

The topographic wetness index (TWI), reflecting topographic-controlled lateral water distribution (Quinn *et al*., 1995), was calculated with the System for Automated Geoscientific Analyse (SAGA) Geographic Information System (GIS) software (http://www.saga-gis.org/en/index.html).

The solar radiation index (SRI), reflecting topographic (slope and aspect) impacted incoming solar radiation (DEM used as only input in this study) and thus impacting evapotranspiration (Moore *et al*., 1991), was calculated with ARCGIS 9.3 (ESRI Inc., Redlands, CA, USA; 2008).

Methods

We conducted conventional statistical analysis with SPSS 15.0 (SPSS Inc., Chicago, IL, USA; 1989–2006) and Microsoft Excel 2003 (Microsoft Corporation, Redmond, WA, USA; 1985–2003) and spatial and geostatistical analysis with ARCGIS 9.3 (ESRI Inc., Redlands, CA, USA; 2008).

The sample semivariogram, $\gamma_s(h)$, which is half the average squared difference between the values of data pairs (Western *et al*., 2004), was estimated from

$$\gamma_s(h) = \frac{1}{2N(h)} \sum_{ij} \left(\theta_i - \theta_j\right)^2 \tag{1}$$

where h is the lag, $N(h)$ is the number of data pairs located in a given lag bin, and θ_i and θ_j are the soil moisture values at site i and j, respectively. We estimated the omnidirectional semivariogram as done by Western *et al*. (2004).

The exponential semivariogram model with nugget as intercept was selected to fit all of the sample semivariogram in this study. The mathematical function is as follows:

$$\gamma_e(h) = c0 + c1(1 - \exp(-h/r)) \tag{2}$$

$\gamma_e(h)$ is the fitted semivariogram, $c0$ is the nugget, $c1$ is the partial sill and r is the spatial correlation length. This model reaches its sill ($c0 + c1$) asymptotically, with the practical range $3r$, named as the spatial correlation range in this study. If the separation distance between two sites is larger than $3r$, it means no spatial correlation between the two sites exists. The quality of the semivariogram fitting was assessed using coefficient of determination (R^2) as follows:

$$R^2 = 1 - \frac{\sum (r_e(h) - r_s(h))^2}{\sum \left(r_s(h) - r_s(\bar{h})\right)^2} \tag{3}$$

$\overline{r_s(h)}$ is the average value of the sample semivariogram.

RESULTS AND DISCUSSION

Converting ground measured to remotely sensed soil moisture

Figure 2 shows the daily (averaged from the 30-min values) observed surface soil moisture time series at the meteorological tower location. From Figure 2, high soil moisture was observed in winter and spring, whereas lower values occurred in summer. Three types of phases can be identified: a steady wet phase (January to May), a steady

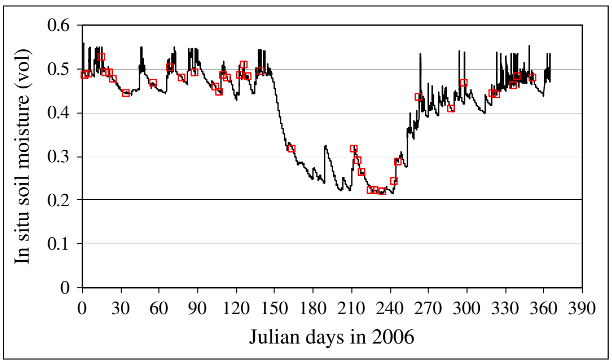

Figure 2. Daily dynamics of the *in situ* soil moisture (black continuous series). The square symbols are used to point out on which day the satellite images were selected.

Table I. Statistical and geostatistical descriptions on the remotely sensed soil moisture in 2006

DOY	Date (MMDD)	Time (HH:MM)	Mean	Standard deviation	Statistical analysis			Geostatistical analysis		
					Coefficient of variation (%)	Nugget ($c0$)	Partial sill ($c1$)	Nugget ratio (%)	Range (m)	R^2
2	0102	22:13–22:14	0.427	0.059	14	0.0018	0.0018	50	540	0.623
5	0105	10:56–10:57	0.401	0.080	20	0.0032	0.0033	49	845	0.847
15	0115	22:05–22:06	0.463	0.038	8	0.0009	0.0007	57	941	0.545
18	0118	10:47–10:48	0.361	0.099	27	0.0033	0.0064	34	523	0.744
21	0121	10:53–10:54	0.380	0.090	24	0.0050	0.0034	60	1088	0.832
24	0124	10:58–10:59	0.422	0.076	18	0.0032	0.0025	56	986	0.867
34	0203	10:44–10:45	0.270	0.127	47	0.0073	0.0092	44	550	0.741
56	0225	10:53–10:54	0.368	0.106	29	0.0044	0.0071	38	775	0.911
69	0310	10:44–10:45	0.317	0.124	39	0.0094	0.0068	58	1658	0.775
78	0319	11:01–11:02	0.440	0.060	14	0.0018	0.0020	47	944	0.822
88	0329	10:47–10:48	0.296	0.140	47	0.0064	0.0127	33	637	0.831
104	0414	10:44–10:45	0.222	0.132	59	0.0086	0.0094	48	862	0.834
107	0417	22:13–22:14	0.290	0.126	43	0.0067	0.0089	43	373	0.570
110	0420	10:56–10:57	0.325	0.127	39	0.0055	0.0107	34	544	0.808
113	0423	11:01–11:02	0.370	0.105	28	0.0030	0.0078	28	530	0.882
123	0503	22:10–22:11	0.346	0.109	31	0.0050	0.0070	42	573	0.821
126	0506	10:53–10:54	0.266	0.143	54	0.0094	0.0109	46	792	0.884
129	0509	10:59–11:00	0.325	0.127	39	0.0074	0.0080	48	810	0.839
139	0519	22:07–22:08	0.377	0.092	24	0.0043	0.0040	51	559	0.791
164	0613	22:21–22:22	0.191	0.126	66	0.0097	0.0060	62	663	0.709
212	0731	22:13–22:14	0.359	0.087	24	0.0039	0.0032	55	314	0.351
215	0803	10:56–10:57	0.273	0.122	45	0.0073	0.0080	48	820	0.916
218	0806	11:02–11:03	0.376	0.087	23	0.0039	0.0034	53	613	0.833
225	0813	22:05–22:06	0.274	0.115	42	0.0078	0.0054	59	416	0.562
228	0816	22:11–22:12	0.322	0.105	33	0.0074	0.0041	64	1335	0.844
234	0822	22:22–22:23	0.283	0.110	39	0.0065	0.0056	54	441	0.677
244	0901	22:07–22:08	0.363	0.089	25	0.0052	0.0028	64	734	0.670
247	0904	10:50–10:51	0.234	0.124	53	0.0077	0.0065	54	745	0.812
263	0920	10:47–10:48	0.323	0.107	33	0.0055	0.0056	49	754	0.884
288	1015	11:02–11:03	0.409	0.079	19	0.0030	0.0033	47	865	0.854
298	1025	10:47–10:48	0.362	0.082	23	0.0033	0.0034	49	644	0.812
320	1112	10:56–10:57	0.385	0.084	22	0.0027	0.0046	37	569	0.850
323	1119	11:01–11:02	0.435	0.060	14	0.0018	0.0018	50	1228	0.861
336	1202	10:53–10:54	0.406	0.063	16	0.0019	0.0022	46	570	0.883
352	1218	10:50–10:51	0.364	0.089	24	0.0037	0.0042	47	561	0.783

MMDD, month and day; HH:MM, hour and minute; DOY, day of year (2006); R^2, coefficient of determination.

dry phase (July and August) and transient phases (from wet to dry in June, and from dry to wet in the period of September to November). In Figure 2, we also show the date when the satellite images are selected for this study. We can find that the selected remote sensing data sets (even though they are at multiday intervals) span all of the phases, and thus are representative of most of the soil wetness regimes in this study area.

From Figure 3a, we found that the backscatter coefficient (from the remote sensing image) is a good estimator ($R^2 > 0.90$) of *in situ* soil moisture. The root mean square error is 0.042 in this study comparable with 0.04–0.07 of other studies (Loew *et al.*, 2006 and references therein). This suggests that the cubic function is applicable for this humid region with observed soil moisture ranging from 0.219 to 0.525 $m^3 m^{-3}$, and its mean value and standard deviation are 0.422 and 0.096 $m^3 m^{-3}$, respectively. According to Figure 3b, the simulated soil moisture with this empirical function applied is underestimated. The simulated soil moisture spatial distribution maps were shown in Figure 1b and c (as an example for wet and dry conditions).

Statistical analysis of remotely sensed soil moisture

The temporal evolution of spatially averaged soil moisture for the whole catchment is shown in Figure 4. It reflects the summer trough of low soil moisture, but the contrasting pattern of dry and wet season is not as distinct as the time series of *in situ* measured soil moisture (Figure 2). This is because the remotely sensed measurements are intermittent in time (Table I) and averaged in space over 15 km^2, whereas the *in situ* observations are 30-min values integrated over a day for one site.

Most of the remotely sensed soil moisture data sets (31 of 35 data sets) in this study are negatively skewed (Kolmogorov–Smirnov test at 0.05 significance level; also see the negative skewness in Figure 5). This is in disagreement with the finding by Brocca *et al.* (2010) who found that most of their field measured soil moisture data can be described by a normal distribution. It might be that they used a limited number (30 for each site) of field measurements within smaller dimensions (60×50 m at each site). With extensive field measurements for both dry and wet conditions at six distinct spatial scales ranging from 2.5 to 50 km, Famiglietti *et al.* (2008) found that the distribution is negatively skewed for wet environments but positively skewed for dry environments. Similar to the results in the study by Famiglietti *et al.* (2008), the skewness (negative value) in our study decreased with

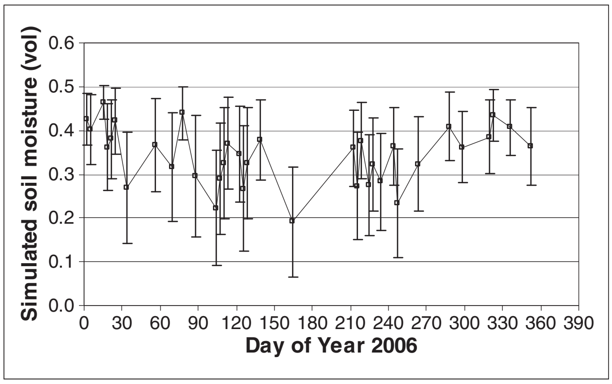

Figure 4. Temporal dynamics of spatial-averaged remotely sensed soil moisture (mean ± one standard deviation).

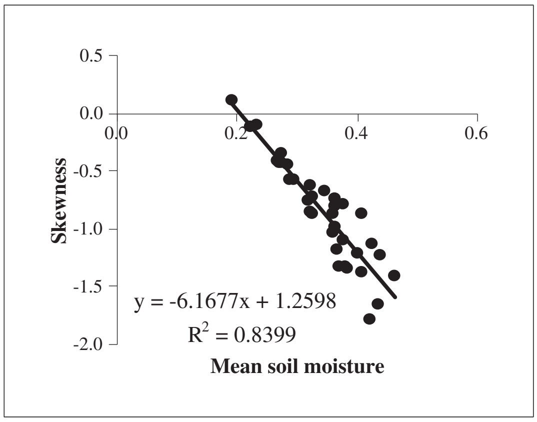

Figure 5. The relationship between skewness of remotely sensed soil moisture and mean soil moisture.

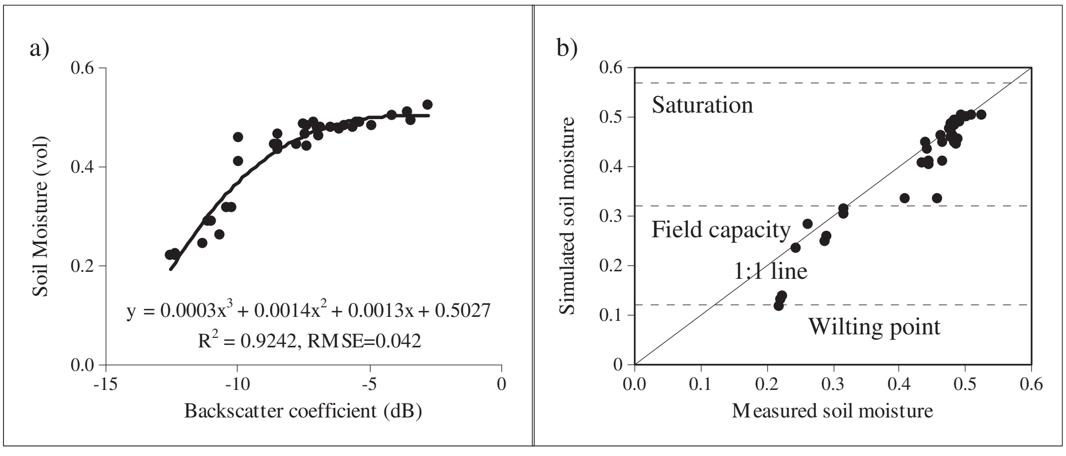

Figure 3. a) The relationship between soil moisture (*in situ* measured) and backscatter coefficient (from remote sensing images), and b) simulated versus measured soil moisture.

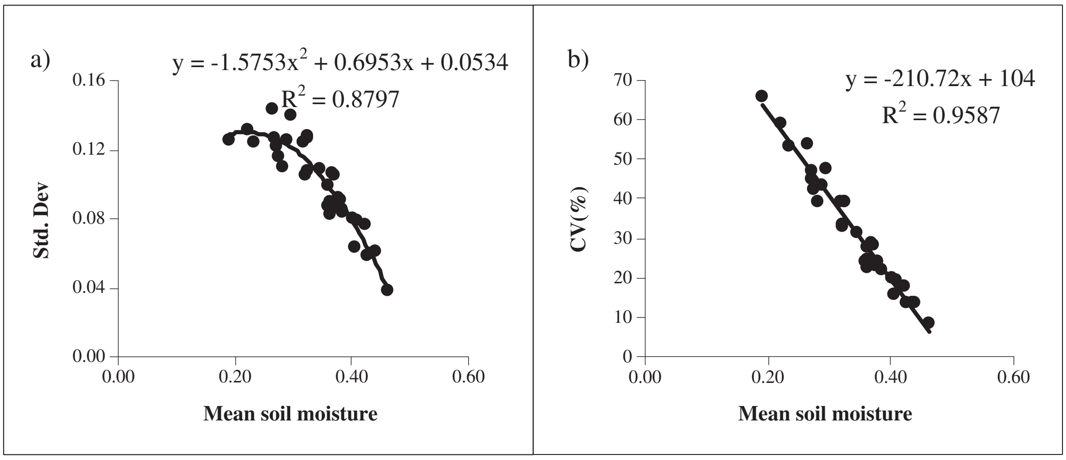

Figure 6. The relationships between mean soil moisture value and a) standard deviation (Std. Dev), and b) coefficient of variation (CV).

increasing spatial mean soil moisture, and the normal distribution (skewness around 0) is at the mean soil moisture of 0.20 (see Figure 5). For another humid area in Iowa, USA, Das and Mohanty (2008) found that polarimetric scanning radiometer–based remotely sensed surface (0–5 cm) soil moisture was also not a normal distribution. The statistical distribution of the soil moisture field thus seems dependent on the scale extent of specific cases (Ryu and Famiglietti, 2005).

The absolute spatial variation (standard deviation) is a quadratic function (upward convex curve) of the spatial mean value but mainly concentrated in the decreasing part of the curve (Figure 6a). The decreasing trend between standard deviation and mean values in humid environments was already shown in the study by Brocca *et al*. (2007) who analysed different studies in different climatic regions. From field observations at different scales, Famiglietti *et al*. (2008) also found variability in soil moisture, initially increasing with increasing soil moisture (at dry conditions), and then decreasing (at wet conditions) beyond some soil moisture threshold. Many other studies also identified and explained this point with model simulations. For example, Vereecken *et al*. (2007) demonstrated that the parameters of the soil water retention characteristic and their variability can explain the relationship between standard deviation and mean soil moisture, and they also found (in a simulation study) for 11 soil texture classes that the standard deviation peaked at mean soil moisture values between 0.17 and 0.23. In our study, the corresponding value was 0.22. Pan and Peters-Lidard (2008) demonstrated that soil texture controlled the relationship between variance and mean soil moisture, and the soil moisture variance peaked at mean soil moisture values from 0.20 to 0.25 for different cases. At a temperate site, Lawrence and Hornberger (2007) found that at low mean soil moisture, the variability is controlled by wilting point; at intermediate mean soil moisture, the variability is controlled by soil hydraulic conductivity; and at high soil moisture, the variability is controlled by porosity. As for the relative variability (coefficient of variation) in this study, it linearly decreased with spatial mean soil moisture (Figure 6b). Many other studies have also found similar decreasing trend (Choi *et al*., 2007; Famiglietti *et al*., 2008; Brocca *et al*., 2010; Mascaro and Vivoni, 2010).

Geostatistical analysis of remotely sensed soil moisture

There is no good relationship between the spatial correlation range and the mean soil moisture (Figure 7a). At another humid area in New Zealand, Western *et al*. (2004) also found no correlation between spatial correlation range and mean soil moisture but found the correlation for the dry sites in Australia. According to Table I, the typical spatial correlation range was 554–854 m, beyond which (the distance between any two sites) no spatial dependence exists for the soil moisture field any more. Most of the nugget ratios [nugget ($c0$) divided by the sum of partial sill (c1) and nugget ($c0$)] were concentrated from 45% (25% percentile) to 55% (75% percentile) with the median value of 49%, which indicated that the spatial dependence of soil moisture field in this area is moderate (Cambardella *et al*., 1994). The relationship (Figure 7b) between nugget ratio and mean soil moisture suggested that relatively lower nugget ratios (therefore good spatial structure of soil moisture field) mainly occurred at the middle soil moisture values.

For all of the cases in this study (Table I), the sample semivariograms (not shown) can reach a certain plateau, which suggests that the remotely sensed soil moisture field was stationary. This is also why we still used the geostatistical analysis method for this study although the variable (soil moisture) is not normally distributed (negative skewness, see Figure 5). Most of these cases had a high coefficient of determination (median value at 0.822, see Table I), demonstrating that the exponential model can provide a good match to the shape of the sample semivariogram, and therefore can be used as a confident estimator of the characteristics of the remotely sensed measured soil moisture field. Western *et al*. (2004) using field measurements for dry conditions in Australia and for wet conditions in New Zealand also found this aspect. The coefficients of determination of the fitted exponential functions for the sample semivariogram are not well correlated with the spatial mean soil moisture (Figure 7c). The worst

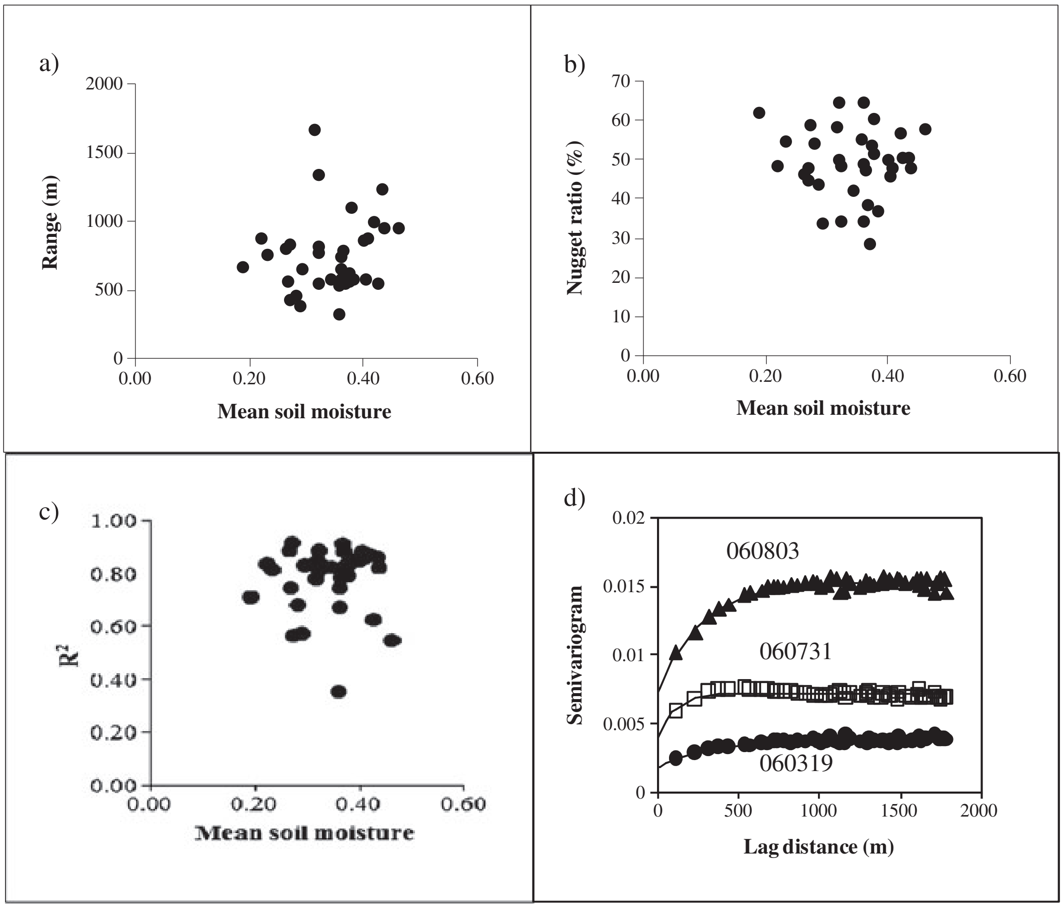

Figure 7. a) The spatial correlation range versus mean soil moisture, b) the nugget ratio versus mean soil moisture, c) coefficient of determination (R^2) versus mean soil moisture and d) sample and exponentially fitted semivariograms for the images on 19 March (060319), 31 July (060731) and 3 August (060803) in 2006, respectively.

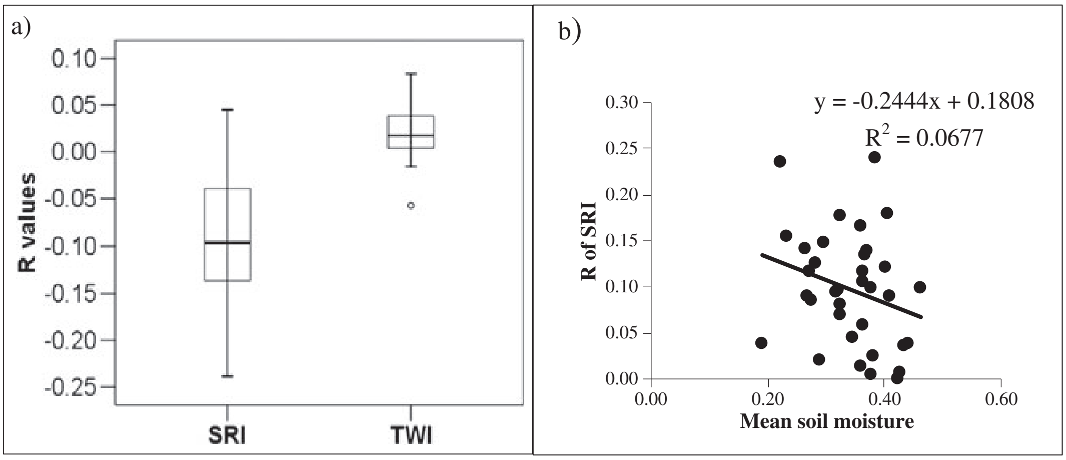

Figure 8. a) The boxplot for the correlation coefficients (R) of solar radiation (SRI) and topographic wetness index (TWI) with soil moisture, and b) the correlation coefficient (R) of solar radiation index (SRI) with soil moisture versus mean soil moisture.

(31 July), moderate (19 March) and best (3 A1 August) fitting cases are shown in Figure 7d.

Correlations between soil moisture and terrain factors

Soil moisture is positively correlated to the topographic wetness index (TWI), but the correlation coefficient (R) is relatively low ranging from 0.004 (25% percentile) to 0.039 (75% percentile) with a median value of 0.017 (Figure 8a). The SRI is negatively correlated with soil moisture, and the R values ranged from −0.137 (25% percentile) to −0.039 (75% percentile) with a median value of −0.097 (Figure 8a). This suggests that SRI plays a relatively more important role in controlling surface soil moisture distribution in this region than TWI, which infers that potential evapotranspiration rather than lateral flow controls the surface soil moisture distribution. In many previous studies (Western *et al*., 2004; De Lannoy *et al*., 2006; Brocca *et al*., 2007), the lateral flow played a more important role in controlling soil moisture spatial distribution, but, as stated by Western *et al*. (2004), the processes controlling soil moisture distribution can change between regions and over time with catchment soil moisture status. Moreover, we found that the absolute R values for SRI had a decreasing trend with spatial mean soil moisture (Figure 8b) suggesting that the relationship between soil moisture and SRI was closer at the dry end of the soil moisture distribution. This may indicate that soil moisture become a limiting factor for evapotranspiration with the progress of soil drying.

CONCLUSIONS

This study shows that the backscatter coefficient acquired from ENVISAT/ASAR WS image is a good estimator of the surface (top 5 cm) soil moisture. The spatial variation (standard deviation and coefficient of variance) of the remotely sensed soil moisture decreased with increasing mean soil moisture for this temperate-humid catchment. The spatial dependence of the remotely sensed soil moisture field was moderate, and the exponential model accurately fitted the sample semivariogram. This study provides important information for soil moisture monitoring at catchment scale. However, there are also some uncertainties in this study: (1) pixel size influences the relationship between *in situ* soil moisture data and backscatter coefficients of remote sensing data set; (2) although there are uniform land cover and soil type in the whole catchment, the heterogeneity of soil properties still affects the applicability of the established relationship at one location to another.

ACKNOWLEDGEMENTS

This study was funded by the Irish Environmental Protection Association (EPA) under the Science Technology Research & Innovation for the Environment (STRIVE) Programme 2007–2013 (*SoilH*: Interactions of soil hydrology, land use and climate change and their impact on soil quality; 2007-S-SL-1-S1). The ENVISAT/ASAR data sets were provided by the European Space Agency (ESA) through the project 6875.

Thanks to anonymous reviewers for their constructive comments.

REFERENCES

Albertson JD, Kiely G. 2001. On the structure of soil moisture time series in the context of land surface models. *Journal of Hydrology* **243**: 101–119.

Baup F, Mougin E, De Rosnay P, Timouk F, Chenerie I. 2007a. Surface soil moisture estimation over the AMMA Sahelian site in Mali using ENVISAT/ASAR data. *Remote Sensing of Environment* **109**: 473–481.

Baup F, Mougin E, Hiernaux P, Lopes A, De Rosnay P, Chenerie I. 2007b. Radar signatures of Sahelian surfaces in Mali using ENVISAT-ASAR data. *IEEE Transactions on Geoscience and Remote Sensing* **44**(7): 2354–2363.

Bell JE, Sherry R, Luo Y. 2010. Changes in soil water dynamics due to variation in precipitation and temperature: an ecohydrological analysis in a tallgrass prairie. *Water Resources Research* **46**: W03523.

Brocca L, Melone F, Moramarco T, Morbidelli R. 2010. Spatial-temporal variability of soil moisture and its estimation across scales. *Water Resources Research* **46**: W02516.

Brocca L, Morbidelli R, Melone F, Moramarco T. 2007. Soil moisture spatial variability in experimental areas of central Italy. *Journal of Hydrology* **333**: 356–373.

Cambardella CA, Moorman TB, Nocak JM, Parkin TB, Karlen DL, Turco RF, Konopka AE. 1994. Field-scale variability of soil properties in central Iowa soils. *Soil Science Society of America Journal* **58**: 1501–1511.

Choi M, Jacobs JM, Cosh MH. 2007. Scaled spatial variability of soil moisture fields. *Geophysical Research Letters* **34**: L01401.

Das NN, Mohanty BP. 2008. Temporal dynamics of PSR-based soil moisture across spatial scales in an agricultural landscape during SMEX02: a wavelet approach. *Remote Sensing of Environment* **112**: 522–534.

De Lannoy GJM, Verhoest NEC, Houser PR, Gish TJ, Meirvenne MV. 2006. Spatial and temporal characteristics of soil moisture in an intensively monitored agricultural field (OPE^3). *Journal of Hydrology* **331**: 719–730.

Famiglietti JS, Ryu D, Berg AA, Rodell M, Jackson TJ. 2008. Field observations of soil moisture variability across scales. *Water Resources Research* **44**: W01423.

Jackson TJ, Cosh MH, Rajat Bindlish, Starks PJ, Bosch DD, Seyfried M, Goodrich DC, Moran MS, Du J. 2010. Validation of advanced microwave scanning radiometer soil moisture products. *IEEE Transactions on Geoscience and Remote Sensing* DOI: 10.1109/TGRS.2010.2051035.

Jacobs JM, Hsu EC, Choi M. 2010. Time stability and variability of electronically scanned thinned array radiometer soil moisture during Southern Great Plains hydrology experiments. *Hydrological Processes* **24**: 2807–2819.

Kim DG, Mishurov M, Kiely G. 2010. Effect of increased N use and dry periods on N_2O emission from a fertilized grassland. *Nutrition Cycle Agroecosystem* DOI: 10.1007/s10705-010-9365-5.

Koster RD, Mahanama SPP, Livneh B, Lettenmaier DP, Reichle RH. 2010. Skill in streamflow forecasts derived from large-scale estimates of soil moisture and snow. *Nature Geoscience* **3**: 613–616.

Lawrence JE, Hornberger GM. 2007. Soil moisture variability across climate zones. *Geophysical Research Letters* **34**: L20402.

Loew A, Ludwig R, Mauser W. 2006. Derivation of surface soil moisture from ENVISAT ASAR wide swath and image mode data in agricultural areas. *IEEE Transactions on Geoscience and Remote Sensing* **44**(4): 889–899.

Mahanama SPP, Koster RD, Reichle RH, Zubair L. 2008. The role of soil moisture initialization in subseasonal and seasonal streamflow prediction – a case study in Sri Lanka. *Advances in Water Resources* **31**: 1333–1343.

Mascaro G, Vivoni ER. 2010. Statistical and scaling properties of remotely-sensed soil moisture in two contrasting domains in the North American monsoon region. *Journal of Arid Environments* **74**: 572–578.

Mladenova I, Lakshmi V, Wagner W. 2010. Validation of ASAR global monitoring mode soil moisture product using the NAFE'05 data set. *IEEE Transactions on Geoscience and Remote Sensing*. DOI: 10/1109/TGRS.2010.2040746.

Montaldo N, Albertson JD, Mancini M, Kiely G. 2001. Robust simulation of root zone soil moisture with assimilation of surface soil moisture. *Water Resources Research* **37**(12): 2889–2900.

Moore ID, Grayson RB, Ladson AR. 1991. Digital terrain modelling, a review of hydrological, geomorphological and biological applications. *Hydrological Processes* **5**: 3–30.

Moran MS, McElroy S, Watts JM, Peters Lidard CD. (2006). *Radar Remote Sensing for Estimation of Surface Soil Moisture at the Watershed Scale. Chapter 5. Modelling and Remote Sensing in Agriculture (US and Mexico)*. Richardson CW, Baez-Gonzales AS, Tiscareno M, (eds). INIFAP Publ: Aquascalientes, Mexico. Oct. 2006. ch. 7., 91–106.

Pathe C, Wagner W, Sabel D, Doubkova M, Basara JB. 2009. Using ENVISAT ASAR global mode data for surface soil moisture retrieval over Oklahoma, USA. *IEEE Transactions on Geoscience and Remote Sensing* **47**(2): 468–480.

Pan F, Peters-Lidard CD. 2008. On the relationship between mean and variance of soil moisture fields. *Journal of the American Water Resources Association* **44**(1): 235–242.

Pumo D, Viola F, Noto LV. 2010. Climate changes' effects on vegetation water stress in Mediterranean areas. *Ecohydrology* **3**: 166–176.

Quinn PF, Beven KJ, Lamb R. 1995. The ln(α/tanβ) index: how to calculate it and how to use it within the Topmodel framework. *Hydrological Processes* **9**:161–182.

Rodriguez-Iturbe I, Vogel GK, Rigon R. 1995. On the spatial organization of soil moisture fields. *Geophysical Research Letters* **22**(20): 2757–2760.

Ryu D, Famiglietti JS. 2005. Characterization of footprint-scale surface soil moisture variability using Gaussian and beta distribution functions during the Southern Great Plains 1997 (SGP97) hydrology experiment. *Water Resources Research* **41**: W12433.

Scanlon TM, Kiely G. 2003. Ecosystem-scale measurements of nitrous oxide fluxes for an intensely grazed, fertilized grassland. *Geophysical Research Letters* **30**: 1852.
Scanlon TM, Kiely G, Xie Q. 2004. A nested catchment approach for defining the hydrological controls on non-point phosphorus transport. *Journal of Hydrology* **291**: 218–231.
Teuling AJ, Seneviratne SI, Stocklil R, Reichstein M, Moors E, Ciais P, Luyssaert S, van den Hurk B, Ammann C, Bernhofer C, Dellwik E, Gianelle D, Gielen B, Grunwald T, Klumpp K, Montagnani L, Moureaux C, Sottocornola M, Wohlfahrt G. 2010. Contrasting response of European forest and grassland energy exchange to heatwaves. *Nature Geoscience* **3**: 722–727.
Tietjen B, Jeltsch F, Zehe E, Classen N, Groengroeft A, Schiffers K, Oldel J. 2010. Effects of climate change on the coupled dynamics of water and vegetation in drylands. *Ecohydrology* **3**: 226–237.
Vereecken H, Kamai T, Harter T, Kasteel R, Hopmans J, Vanderborght J. 2007. Explaining soil moisture variability as a function of mean soil moisture: a stochastic unsaturated flow perspective. *Geophysical Research Letters* **34**: L22402.
Western AW, Zhou SL, Grayson RB, McMahon TA, Bloschl G, Wilson DJ. 2004. Spatial correlation of soil moisture in small catchments and its relationship to dominant spatial hydrological processes. *Journal of Hydrology* **286**: 113–134.
Zribi M, Baghdadi N, Holah N, Fafin O. 2005. New methodology for soil surface moisture estimation and its application to ENVISAT-ASAR multi-incidence data inversion. *Remote Sensing of Environment* **96**: 485–496.
Zribi M, Chahbi A, Shabou M, Lili-Chabaane Z, Duchemin B, Baghdadi N, Chehbouni A. 2010. Multi-scale estimation of surface moisture in a semi-arid region using ENVISAT ASAR radar data. *Hydrology Earth System Science Discussion* **7**: 8045–8089.

